Pharmaceutical Research, Vol. 23, No. 7, July 2006 (© 2006)
DOI: 10.1007/s11095-006-0285-7

Research Paper

Establishment and Characterization of the Transformants Stably-Expressing *MDR1* Derived from Various Animal Species in LLC-PK$_1$

Toshiyuki Takeuchi,[1,4] Sumie Yoshitomi,[2] Tomoaki Higuchi,[1] Keiko Ikemoto,[2] Shin-Ichi Niwa,[2] Takuya Ebihara,[1] Miki Katoh,[3] Tsuyoshi Yokoi,[3] and Satoru Asahi[1]

Received January 6, 2006; accepted March 1, 2006

Purpose. Stable transformants expressing human *multidrug resistance 1* (*MDR1*), monkey *MDR1*, canine *MDR1*, rat *MDR1a*, rat *MDR1b*, mouse *mdr1a*, and mouse *mdr1b* in LLC-PK$_1$ were established to investigate species differences in P-glycoprotein (P-gp, ABCB1) mediated efflux activity.
Methods. The seven cDNAs of *MDR1* from five animals were cloned, and their transformants stably expressing the series of *MDR1* in LLC-PK$_1$ were established. Transport studies of clarithromycin, daunorubicin, digoxin, erythromycin, etoposide, paclitaxel, propranolol, quinidine, ritonavir, saquinavir, verapamil, and vinblastine were performed by using these cells, and efflux activity was compared among the species.
Results. Except for propranolol, all compounds showed efflux activity in all transformants, and were judged to be substrates of P-gp. There were slight interspecies and interisoforms differences in the substrate recognition. However, the efflux ratio among the series of the *MDR1* stably expressing cells showed good correlation as represented between human and monkey MDR1, and poor correlation as represented between human MDR1 and mouse mdr1a, and human and canine MDR1.
Conclusions. Results in the present study indicate that all *MDR1* stably expressing cells have efflux activity for various P-gp substrates, and that interspecies differences and similarities of the P-gp substrate efflux activity may exist.

KEY WORDS: LLC-PK$_1$; multidrug resistance 1 (MDR1); P-glycoprotein (P-gp, ABCB1); species difference; stably expressing cell.

INTRODUCTION

P-glycoprotein (P-gp, ABCB1), which was originally found in multidrug resistant (MDR) tumor cells as an anticancer drug efflux transporter (1), is also highly expressed in normal tissues. This transporter is localized on the columnar epithelial cells of the intestine, the canalicular surface of the hepatocytes in the liver, the apical surface of the epithelial cells of the proximal tubules in the kidneys, and the luminal surface of the capillary endothelial cells in the brain (2). The anatomical localization of P-gp expression suggests that the efflux transporter can functionally protect the body against toxic xenobiotics by excreting these compounds into the intestinal lumen, bile, and urine, and by preventing their accumulation in the brain (3).

Recently, it was shown that P-gp can reduce the oral bioavailability (BA) of its substrates by attenuating intestinal absorption and by potentially enhancing intestinal metabolism of substrates, which are subject to first-pass intestinal metabolism (4–6). Furthermore, inter- and intrapatient variation in intestinal P-gp expression, possible drug–drug interactions involving coadministered P-gp substrates, inhibitors, or inducers, and dose-dependent absorption due to saturation of P-gp activity can lead to unpredictable abnormalities in the disposition of P-gp substrates (7–9). Therefore, estimation of P-gp contribution to the pharmacokinetics is important for the research and development of a new drug.

There are two practical problems in determining P-gp contribution to the pharmacokinetics. The first is species differences. There have been only a few reports on species differences for P-gp. Although gene knockout mice have been used to evaluate the contribution of P-gps to the pharmacokinetics of drugs (10,11), limited information is available because of species differences. The most obvious species difference for P-gp between rodents and humans is the number of *MDR1*—in that there are two isoforms, *mdr1a* and *mdr1b*, in rats and mice, whereas there is only one in

[1] Development Research Center, Pharmaceutical Research Division, Takeda Pharmaceutical Company Limited, 2-17-85 Juso-Honmachi, Yodogawa-ku, Osaka 532-8686, Japan.
[2] Discovery Research Center, Pharmaceutical Research Division, Takeda Pharmaceutical Company Limited, 2-17-85 Juso-Honmachi, Yodogawa-ku, Osaka 532-8686, Japan.
[3] Department of Graduate School of Medical Science, Kanazawa University, Kakuma, Kanazawa 920-1192, Japan.
[4] To whom correspondence should be addresed. (e-mail: Takeuchi_Toshiyuki@takeda.co.jp)

ABBREVIATIONS: A, apical; B, basolateral; BA, bioavailability; BSA, bovine serum albumin; calcein AM, calcein acetoxymethyl ester; cDNA, complementary DNA; FBS, fetal bovine serum; MDR, multidrug resistance; PBS, phosphate buffered saline; P-gp, P-glycoprotein; RT-PCR, reverse transcriptase polymerase chain reaction.

humans (12). Species differences in functional activity between human P-gp and the two mouse P-gps have also been reported (13,14). Moreover, some reports describe that species differences in the pharmacokinetics of a compound may be caused by those in P-gp function (15,16). The second practical problem is the distinction of transport and metabolism. If a compound is transported by P-gp and also metabolized by a metabolic enzyme, it is difficult to estimate the relative contribution for alteration of the pharmacokinetic parameters in a drug–drug interaction study. Some compounds are known to be substrates of both P-gp and CYP3A4, and there are several reports on P-gp-mediated drug–drug interaction (17,18). Overlapping the substrate specificity between P-gp and CYP3A4, and similarities in P-gp and CYP3A4 inhibitors and inducers make it difficult to distinguish the relative contribution of P-gp and CYP3A4 to overall drug interactions. One of the best ways to resolve these two practical problems would be the establishment of a P-gp expression system and the evaluation of P-gp function *in vitro* among the species.

In the present study, we established stable transformants expressing human *MDR1*, monkey *MDR1*, canine *MDR1*, rat *MDR1a*, rat *MDR1b*, mouse *mdr1a*, or mouse *mdr1b*, respectively, and investigated the interspecies and interisoforms differences for MDR1 in terms of P-gp substrate efflux activity by using efflux ratio as a parameter.

MATERIALS AND METHODS

Materials

Vybrant Multidrug Resistance Assay Kit was obtained from Molecular Probes (Eugene, OR, USA); colchicine was obtained from ICN Biochemicals Inc. (Aurora, OH, USA); verapamil was from Sigma-Aldrich (St. Louis, MO, USA); [^{3}H]daunorubicin (162.8 GBq mmol^{-1}), [^{3}H(G)]digoxin (330.0 and 1369.0 GBq mmol^{-1}), [*N*-methyl-^{14}C]erythromycin (1.81 GBq mmol^{-1}), and [*N*-methyl-^{3}H]verapamil hydrochloride (3145.0 GBq mmol^{-1}) were from Perkin-Elmer Life and Analytical Sciences (Boston, MA, USA); DL-[4-^{3}H]propranolol (1221.0 GBq mmol^{-1}) and [G-^{3}H]vinblastine sulfate (248.0 GBq mmol^{-1}) were from Amersham Biosciences UK (Cardiff, UK); D-[1-^{14}C]mannitol (2.035 GBq mmol^{-1}) and [9-^{3}H]quinidine (740 GBq mmol^{-1}) were from American Radiolabeled Chemicals (St. Louis, MO, USA); [methyl-^{3}H]clarithromycin (740.0 GBq mmol^{-1}), [^{3}H]etoposide (24.2 GBq mmol^{-1}), [*o*-benzamido-^{3}H]paclitaxel (1517.0 GBq mmol^{-1}), [^{3}H]ritonavir (103.6 GBq mmol^{-1}), and [^{3}H]saquinavir (103.6 GBq mmol^{-1}) were from Moravek Biochemicals, Inc. (Mercury Lane, Brea, CA, USA); phosphate-buffered saline (PBS) (−) was from Dai-nippon Pharmaceutical Company (Osaka, Japan). All other chemicals and solvents were of the highest grade commercially available.

Cells

LLC-PK$_1$ was obtained from American Type Culture Collection (ATCC, Manassas, VA, USA) and cultured in Medium 199 (Invitrogen, Carlsbad, CA, USA) supplemented with 5% heat-inactivated fetal bovine serum (FBS; Trace Scientific, Melbourne, Australia), 50 units mL^{-1} penicillin, and 50 μg mL^{-1} streptomycin (Invitrogen) in a humidified atmosphere in 5% CO_2–95% air at 37°C. Transformants were cultured in Medium 199 supplemented with 10% FBS, 500 μg mL^{-1} G418 (Invitrogen), 150 ng mL^{-1} colchicine. Mock strain (pcLLC.1) was cultured in Medium 199 supplemented with 10% FBS, 500 μg mL^{-1} G418. LLC-GA5-COL300 (19,20), which was used as a positive control for the human *MDR1* stable transformant, was kindly supplied by Drs. Yusuke Tanigawara and Kazumitsu Ueda. LLC-GA5-COL300 was cultured in Medium 199 supplemented with 10% FBS, 300 ng mL^{-1} colchicine.

Plasmid Construction

The series of *MDR1* complementary DNAs (cDNAs) were cloned via a reverse transcriptase polymerase chain reaction (RT-PCR) by using primers summarized in Table I.

Table I. Sequences of Primers for RT-PCR Analysis

Gene	Primer	Sequence
Human *MDR1*	Sense	5′-TTTTGCTAGCATGGATCTTGAAGGGGACCGCAATG-3′
	Antisense	5′-TTTTGGATCCTTATTATCACTGGCGCTTTGTTCCA-3′
Monkey *MDR1*	Sense	5′-TTTTGCTAGCATGGATCTTGAAGGGGACCGCAATG-3′
	Antisense	5′-TTTTCTCGAGTTATTATCACTGGCGCTTTGCTCCA-3′
Canine *MDR1*	Sense	5′-TTTTGCTAGCATGGATCCTGAAGGAGGCCGTAAGG-3′
	Antisense	5′-TTTTGATATCTTATTACTAGCGCTTTGCTCCAGCC-3′
Rat *MDR1a*	Sense	5′-TTTTGCTAGCATGGAGCTCGAAGAAGACCT-3′
	Antisense	5′-NNNNCTCGAGTCATGAGCGCTTTGCTCCAGCC-3′
Rat *MDR1b*	Sense	5′-TTTTGCTAGCATGGAGTTTGAAGAGGGCCT-3′
	Antisense	5′-TTTTGATATCTTATTATCATGAGCGCTTTGCTCCAG-3′
Mouse *mdr1a*	Sense	5′-TTTTGCTAGCATGGAACTTGAAGAGGACCT-3′
	Antisense	5′-TTTTGATATCTTATTATCATGAGCGCTTTGCTCCAG-3′
Mouse *mdr1b*	Sense	5′-TTTTGCTAGCATGGAGTTTGAAGAGAACCT-3′
	Antisense	5′-TTTTGATATCTTATTATCATGAGCGCTTTGCTCCAGCCTGGACCA-3′
Pig β-actin	Sense	5′-CAGGAGATGGCCACCGCTGCG-3′
	Antisense	5′-TCCTTCTGCATCCTGTCGGCA-3′

The sequence of human *MDR1* referenced GenBank accession no. AF016535; monkey *MDR1* to AF537133; canine *MDR1* to AF536758; rat *MDR1a* to AF257746; rat *MDR1b* to M81855; mouse *mdr1a* to M33581, mouse *mdr1b* to NM_011075. Human *MDR1* was cloned from human small intestine polyA$^+$ RNA (Clontech, Palo Alto, CA, USA), monkey *MDR1* from cynomolgus monkey small intestine total RNA (Unitech, Chiba, Japan), canine *MDR1* from canine small intestine total RNA (Unitech), rat *MDR1a* and *MDR1b* from Rat Liver Quick-clone™ cDNA (Clontech), and mouse *mdr1a* and *mdr1b* from mouse small intestine total RNA (Ori Gene Technologies, Inc., Rockville, MD, USA). The amplified products were cloned into appropriate vector and further ligated into pcDNA3.1(+) (Invitrogen).

Establishment of LLC-PK$_1$ Transformants Stably Expressing *MDR1*

LLC-PK$_1$ (2×10^5 cells) cells were seeded on 24 well plates (Falcon, Franklin Lakes, NJ, USA). After 1 day culture, 2 μg plasmid DNA was transfected by LipofectAMINE 2000 Reagent (Invitrogen). After incubation for 1 day, cells were seeded on 60-mm dishes (Falcon). After incubation for another day, cells were selected for G418 (500 μg mL^{-1}), and resistant colonies were further selected with a medium containing 150 ng mL^{-1} colchicine. Surviving single colonies were selected and MDR1 activity was determined by extrusion of calcein acetoxymethyl ester (calcein AM) followed by transepithelial transport activity of typical P-gp substrates, digoxin and vinblastine. The homogeneity of transformants was ensured by repeated subcloning.

Determination of MDR1 Activity by Extruding Calcein AM

Cells (4×10^4 cells well^{-1}) were seeded on 96-well black view plates (Corning Costar, Corning, NY, USA) and cultured overnight. Cells were incubated for 1 h with or without cyclosporin A (final concentration, 2.5–10 μmol L^{-1}), and then calcein AM (Molecular Probes; final concentration, 2 μmol L^{-1}) was added to the culture medium and incubated for another hour. Calcein retention in the cells was measured as calcein specific fluorescence (excitation and emission of 485 and 538 nm, respectively).

RT-PCR Analysis

LLC-PK$_1$ and its transformants were cultured to semi-confluence and total RNAs were extracted from the cells with RNeasy Mini Kit (Qiagen, Hilden Germany). cDNA was synthesized with the ThermoScript™ RT-PCR System (Invitrogen). β-Actin, human *MDR1*, monkey *MDR1*, canine *MDR1*, rat *MDR1a*, rat *MDR1b*, mouse *mdr1a*, and mouse *mdr1b* cDNA fragments were amplified via KOD Plus DNA Polymerase (Toyobo, Suita, Japan) using the primers summarized in Table I. RT-PCR reaction products were electrophoresed on 1% agarose gel and stained with SYBR Safe™ DNA gel stain (Invitrogen), and stained bands were analyzed by Fluor-S MultiImager (Bio-Rad, Hercules, CA, USA).

Western Blotting Analysis

Cells were grown to 80–90% confluence and lysed in Laemmli sample buffer (Bio-Rad). The cell lysate (2.5×10^4 cells lane^{-1}) was applied on 7.5% polyacrylamide-gel (Bio-Rad) and electrophoresed. The electrophoresed proteins were transcribed to a PVDF membrane (Bio-Rad), and detected by using mouse antihuman MDR1 monoclonal antibody C219 (Calbiochem, La Jolla, CA, USA) as the first antibody and antimouse IgG (H + L) AP conjugate (Bio-Rad) as the second antibody.

MDR1 Transport Activity

The transepithelial transport study was carried out as previously described (21). pcLLC.1 and *MDR1* transformants were seeded on microporous (3 μm) polycarbonate membrane filters (Transwell™; Costar Corp., Cambridge, MA) at a cell density of 5×10^5 or 7.5×10^5 cells cm^{-2}. Cells were cultured on a membrane filter with 1.5 and 0.5 mL of complete medium with colchicine (150 ng mL^{-1}) in the outside and inside of the chamber, respectively, in an atmosphere of 5% CO_2–95% air at 37°C for 4 days. The medium was replaced with fresh medium on the third day after seeding. Transepithelial resistance was measured in each well with a Millicell Ohmmeter (model ERS; Millipore Corp., Bedford, MA, USA). Wells indicating a resistance of 49 Ω cm^2 or greater, after correcting for the resistance obtained in the control blank wells, were used for the transport experiment. Approximately 3 h before the initiation of the transport experiments, the medium in each compartment was replaced with a fresh medium without colchicine. Radioactive compounds were only used for the transport experiments. All compounds were dissolved in dimethylsulfoxide (DMSO), and their solution was added to the medium at a final concentration of 0.5 (v/v)% DMSO. The initial concentration of the compounds was determined based on the specific activity, and the value for [^{3}H]clarithromycin, [^{3}H]daunorubicin, [^{3}H]digoxin, [^{14}C]erythromycin, [^{3}H]etoposide, [^{3}H]paclitaxel, [^{3}H]propranolol, [^{3}H]quinidine, [^{3}H]ritonavir, [^{3}H]saquinavir, [^{3}H]verapamil, and [^{3}H]vinblastine was 5025, 36.7, 12.2, 5100, 5120, 3.9, 48.2, 10.1, 62.7, 69.9, 2.2, and 26.9 nmol L^{-1}, respectively. The medium on the donor side of the monolayers was replaced with a medium containing the test compounds, and the monolayers were then incubated in 5% CO_2–95% air at 37°C. Aliquots from the receiver side (50 μL inside or 150 μL outside) were taken at 0.5, 1, 2, and 3 h. Radioactivity was measured with a liquid scintillation counter (LSC 5100, Aloka, Tokyo, Japan) after the addition of 10 mL scintillation cocktail A (Wako Pure Chemicals, Osaka, Japan). For the intracellular accumulation study, cells were washed with ice-cold PBS (–) immediately after the last sampling. Cells were solubilized overnight with 0.25 mL of 0.3 mol L^{-1} NaOH, and were neutralized with 0.25 mL of 0.3 mol L^{-1} HCl. Radioactivity in 200-μL portions of the aliquots was counted. Protein contents in the cells were measured with Coomassie Plus™ Protein Assay Reagent (Pierce, Rockford, IL, USA) using bovine serum albumin (BSA; Pierce) as a standard. Directional transport was measured in triplicate and presented as the mean ± SD (n = 3).

Inhibition of MDR1 Activity

To examine the inhibitory effects of verapamil on the P-gp-mediated transport, verapamil was added into the medium on both sides of the cell monolayer 3 h before the substrate is added. The inhibitory potencies to the P-gp-mediated transport of 12.2 nmol L^{-1} [^{3}H]digoxin were investigated with 12.5, 25, and 50 μmol L^{-1} verapamil. The paracellular leakage was monitored by the appearance of radioactivity on the receiver side after the addition of [^{14}C]mannitol to the donor side.

Data Analyses

The calculation method for the permeability–surface area (PS) product across the monolayer was previously reported (22) and defined as follows:

$$\text{PS product} = A/t/C_0 \quad (1)$$

where t, A, and C_0 represent incubation time, transport amount of compounds per mg protein of cell monolayer, and initial concentration of compounds in the donor side, respectively. Efflux ratio across the monolayer was defined as follows:

$$\text{efflux ratio} = PS_{B-to-A}/PS_{A-to-B} \quad (2)$$

where $PS_{B\text{-}to\text{-}A}$ and $PS_{A\text{-}to\text{-}B}$ represent PS product in the basolateral (B)-to-apical (A) direction and the A-to-B direction, respectively. In *MDR1* stably expressing cells, the corrected efflux ratio was defined as follows:

$$\text{corrected efflux ratio} = \text{efflux ratio in } \textit{MDR1} \text{ stably expressing cells}/\text{efflux ratio in pcLLC.1} \quad (3)$$

The calculation method for the cell/medium concentration (C/M) ratio was defined as follows:

$$\text{C/M ratio} = A/C_0 \quad (4)$$

where A and C_0 represent the amount of compounds at 3 h in the cells per mg protein of cell monolayer and the initial concentration of compounds in the donor side, respectively.

RESULTS

Establishment of Transformants Expressing *MDR1*

The *MDR1* cDNAs encoding seven subtypes were cloned from cDNA libraries derived from humans, monkeys, dogs, rats, and mice. The amino acid sequences of the cloned cDNAs were identical to those reported. cDNA coded human *MDR1*, monkey *MDR1*, canine *MDR1*, rat *MDR1a*, rat *MDR1b*, mouse *mdr1a*, and mouse *mdr1b* was inserted into pcDNA3.1(+), and designated as human mdr1-10/pcDNA3.1(+)/JM109, primate mdr1-4/pcDNA3.1(+)/JM109, canine mdr1-27/pcDNA3.1(+)/JM109, R1a-104-M1G/pcDNA3.1(+)/Stbl2, rat mdr1b-36/pcDNA3.1(+)/JM109, mouse mdr1a-21-3/pcDNA3.1(+)/Stbl2, and mouse mdr1b-23/pcDNA3.1(+)/JM109, respectively. These plasmids were introduced into LLC-PK_1, and the cells were selected for G418 resistance and further selected in medium containing colchicine. Each G418-colchicine-resistant transformant was assayed for MDR1 expression via determination by the calcein efflux assay, followed by the transcellular transport activities for typical P-gp substrates, digoxin and vinblastine. The selected transformants were designated as hMDR1/LLC.2E2 for human *MDR1* expressing transformant (human MDR1), pMDR1/LLC.1H2 for monkey *MDR1* (monkey MDR1), cMDR1/LLC.1B4 for canine *MDR1* (canine MDR1), rMDR1a/LLC.1E2 for rat *MDR1a* (rat MDR1a), rMDR1b/LLC.1F10 for rat *MDR1b* (rat MDR1b), mmdr1a/LLC.1B1 for mouse *mdr1a* (mouse mdr1a), and mmdr1b/LLC.2H5 for mouse *mdr1b* (mouse mdr1b), respectively. As a mock control, pcDNA3.1(+) was introduced into LLC-PK_1 and named pcLLC.1. Expression of mRNA in each transformant was examined by RT-PCR analysis (Fig. 1). A significant *MDR1* mRNA was detected in the corresponding transformant and no definite RT-PCR product corresponding to *MDR1* mRNA was found in the LLC-PK_1 and pcLLC.1 cells. The sequences of *MDR1* expressed in these trans-

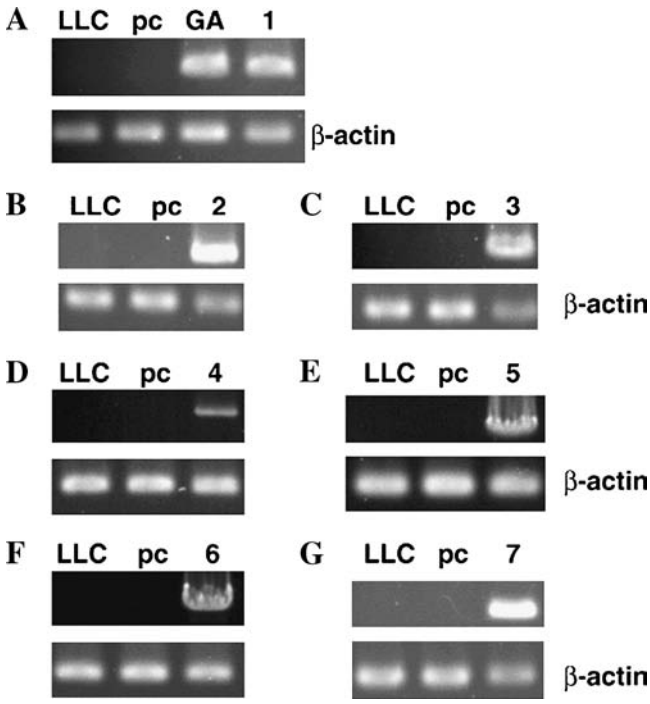

Fig. 1. RT-PCR analysis of *MDR1* mRNA expression in the transformants. Total RNAs were extracted and cDNA was synthesized with ThermoScript RT-PCR system. Fragments of the *MDR1s* and β-actin from various animal species and β-actin were amplified by KOD Plus DNA polymerase. Primers are summarized in Table I. RT-PCR reaction products were electrophoresed on 1% agarose gel and stained with SYBR Safe™ DNA gel stain. (A) Human MDR1, (B) monkey MDR1, (C) canine MDR1, (D) rat MDR1a, (E) rat MDR1b, (F) mouse mdr1a, (G) mouse mdr1b. Lane 1, hMDR1/LLC.2E2; lane 2, pMDR1/LLC.1H2; lane 3, cMDR1/LLC.1B4; lane 4, rMDR1a/LLC.1E2; lane 5, rMDR1b/LLC.1F10; lane 6, mmdr1a/LLC.1B1; lane 7, mmdr1b/LLC.2H5; LLC, LLC-PK_1; pc, pcLLC.1; GA, LLC-GA5-COL300.

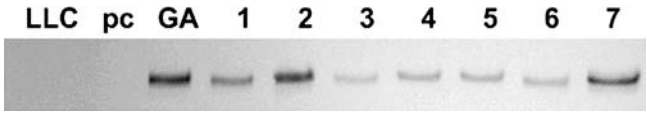

Fig. 2. Western blotting analysis of MDR1 protein in the transformants. Cells were lysed in Laemmli sample buffer. The cell lysate (2.5×10^4 cells lane^{-1}) was applied on 7.5% polyacrylamide-gel and electrophoresed. The electrophoresed proteins were transcribed to a PVDF membrane and detected using mouse antihuman MDR1 monoclonal antibody C219 as first antibody and antimouse IgG (H+L) AP conjugate as second antibody. Lane 1, human MDR1; lane 2, monkey MDR1; lane 3, canine MDR1; lane 4, rat MDR1a; lane 5, rat MDR1b; lane 6, mouse mdr1a; lane 7, mouse mdr1b; LLC, LLC-PK_1; pc, pcLLC.1; GA, LLC-GA5-COL300.

formants were identical to those in introduced cDNAs, respectively. In addition to this, P-gps expressed in these transformants were shown to have almost the same mobility as those in LLC-GA5-COL300, which expresses human MDR1 stably, by Western blot analysis using anti-P-gp monoclonal antibody C219 (Fig. 2). MDR1 activity in each transformant has been stable for more than 1 year. The proliferation rates of these transformants were almost same and the doubling time was around 15 h.

Transcellular Transport and Cellular Accumulation of Digoxin and Vinblastine in *MDR1* Stably Expressing Cells

Figures 3 and 4 show the time profiles for the transcellular transport of digoxin and vinblastine in the series of *MDR1* stably expressing cells and pcLLC.1 cells. In all *MDR1* stably expressing cells, the permeation of both compounds was almost linear up to 3 h after initiation of the transport, and the B-to-A flux of both compounds markedly exceeded the A-to-B flux. In pcLLC.1 cells, smaller polarized transport was also observed. Figure 5 shows the cellular accumulation of digoxin and vinblastine. There was no difference in the accumulation of digoxin between *MDR1* stably expressing cells and pcLLC.1, whereas vinblastine showed less cellular accumulation in all *MDR1* stably expressing cells than pcLLC.1. Accumulation of both compounds in all cells in the A-to-B direction tended to be smaller than in the B-to-A direction.

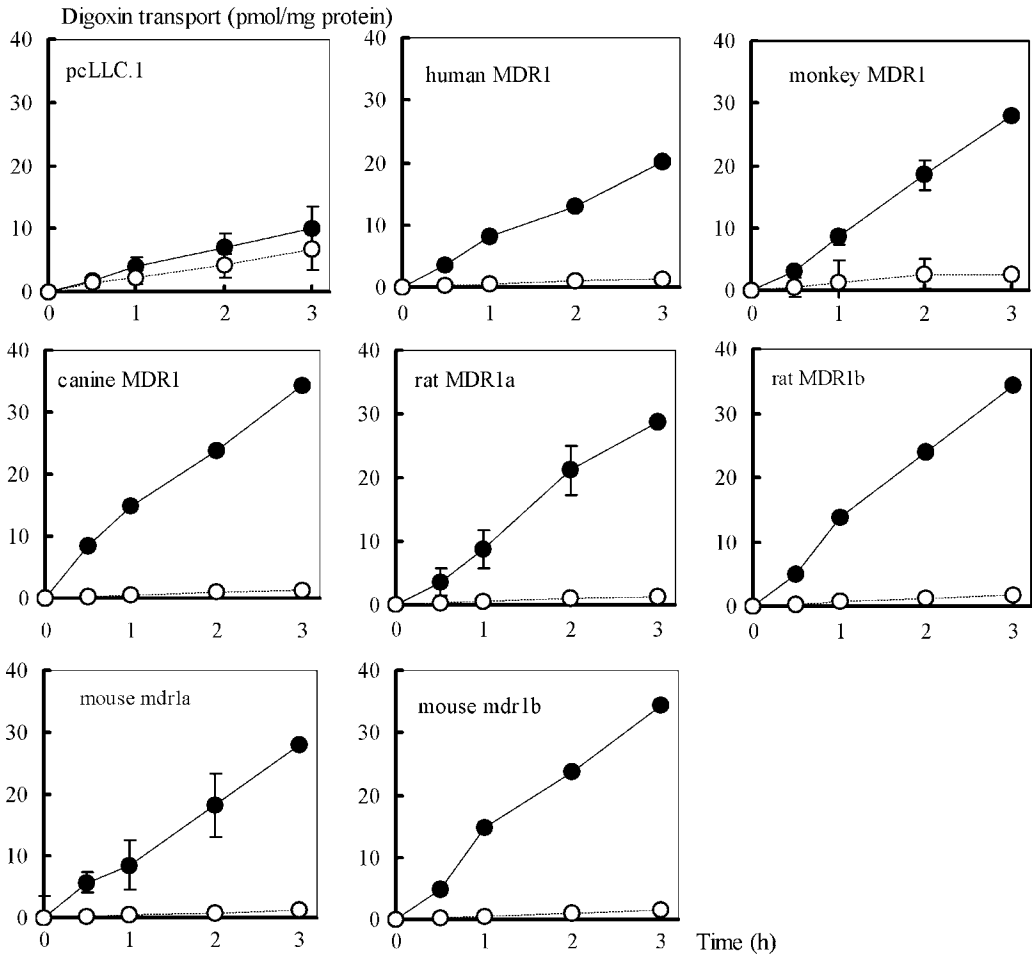

Fig. 3. Transcellular transport of digoxin across *MDR1* stably expressing derived from various animal species and pcLLC.1 cell monolayers. The concentration of digoxin was 12.2 nmol L^{-1}. Open and closed circles represent translocation from A-to-B compartment and B-to-A compartment of digoxin, respectively. Data are shown as mean ± SD (n = 3–9).

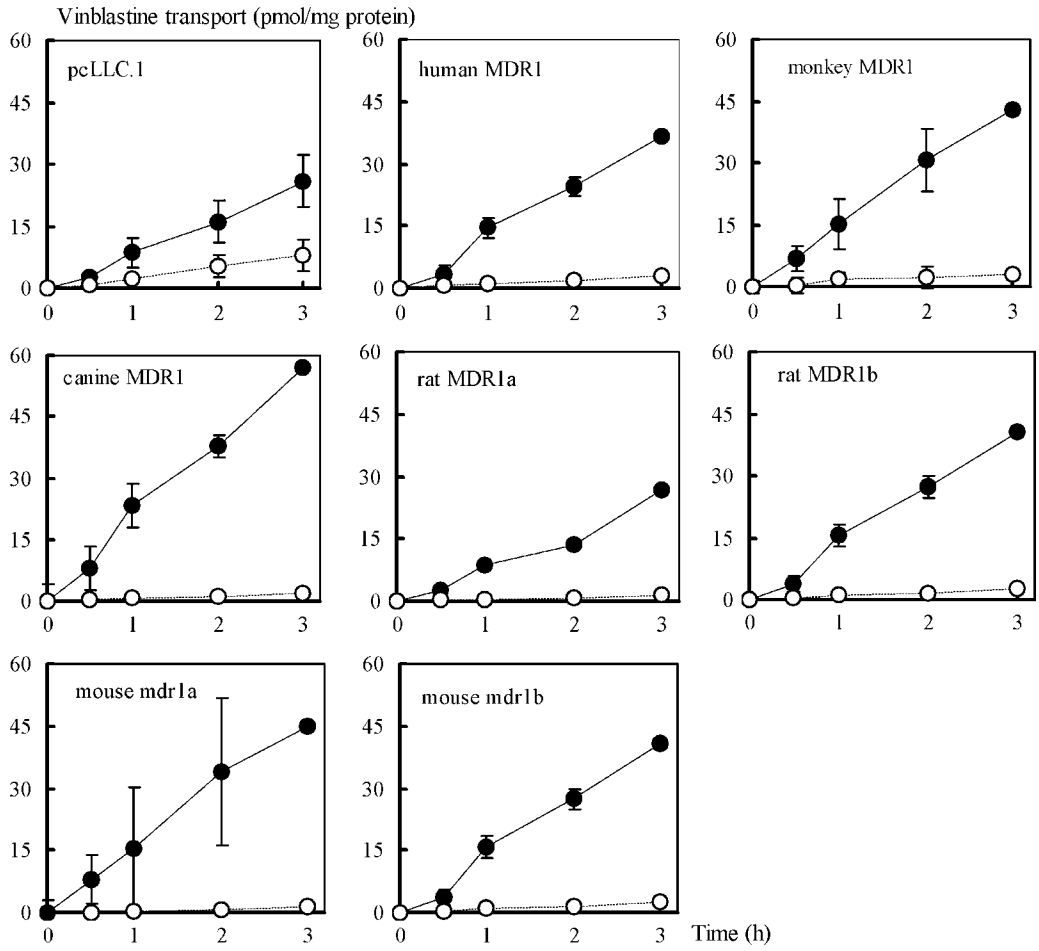

Fig. 4. Transcellular transport of vinblastine across *MDR1* stably expressing derived from various animal species and pcLLC.1 cell monolayers. The concentration of vinblastine was 26.9 nmol L^{-1}. Open and closed circles represent translocation from A-to-B compartment and B-to-A compartment of vinblastine, respectively. Data are shown as mean ± SD (n = 3–9).

Inhibition of Digoxin Transport by Verapamil in Human *MDR1* Stably Expressing Cells

Table II shows the effect of verapamil, which is a known P-gp inhibitor, on digoxin transport. A concentration-dependent inhibition of digoxin transport in both A-to-B and B-to-A directions was detected in human *MDR1* stably expressing cells, whereas transport of digoxin in pcLLC.1 cells did not change. Transport of mannitol, which was used as a paracellular marker, in either of the cells also did not change throughout the experiment (data not shown).

Comparison of Transcellular Transport and Cellular Accumulation Characteristics between Several Compounds

To compare the transport and accumulation characteristics of P-gp substrates in each cell line, transcellular transport studies for clarithromycin, daunorubicin, digoxin, erythromycin, etoposide, paclitaxel, propranolol, quinidine, ritonavir, saquinavir, verapamil, and vinblastine, which are reported to be substrates for efflux transporters, were examined. Results are summarized in Tables III and IV. Because the transport of several compounds was not linear up to 3 h after the initiation of experiments, the PS product, efflux ratio, and corrected efflux ratio for each compound were calculated at the time point when the permeated amounts increased linearly. As a result, various parameters were observed among the compounds. The B-to-A flux for almost all compounds in all *MDR1* stably expressing cells markedly exceeded the A-to-B flux, and the efflux ratios for these compounds are greater than one. Efflux ratios for propranolol were almost one, and efflux activity was hardly detectable in any of the *MDR1* stably expressing cells. Although efflux ratios for erythromycin were comparatively high in all *MDR1* expressing cells, the values were not different compared with that for pcLLC.1 cells. Variety in cellular accumulation was also observed among the compounds. Clarithromycin, daunorubicin, erythromycin, paclitaxel, ritonavir, saquinavir, and vinblastine showed reduced cellular accumulation in all *MDR1* stably expressing cells than in the pcLLC.1 cells, whereas other compounds showed no differences. Accumulation of almost all compounds in all cells in the A-to-B direction tended to be less than that in the B-to-A direction.

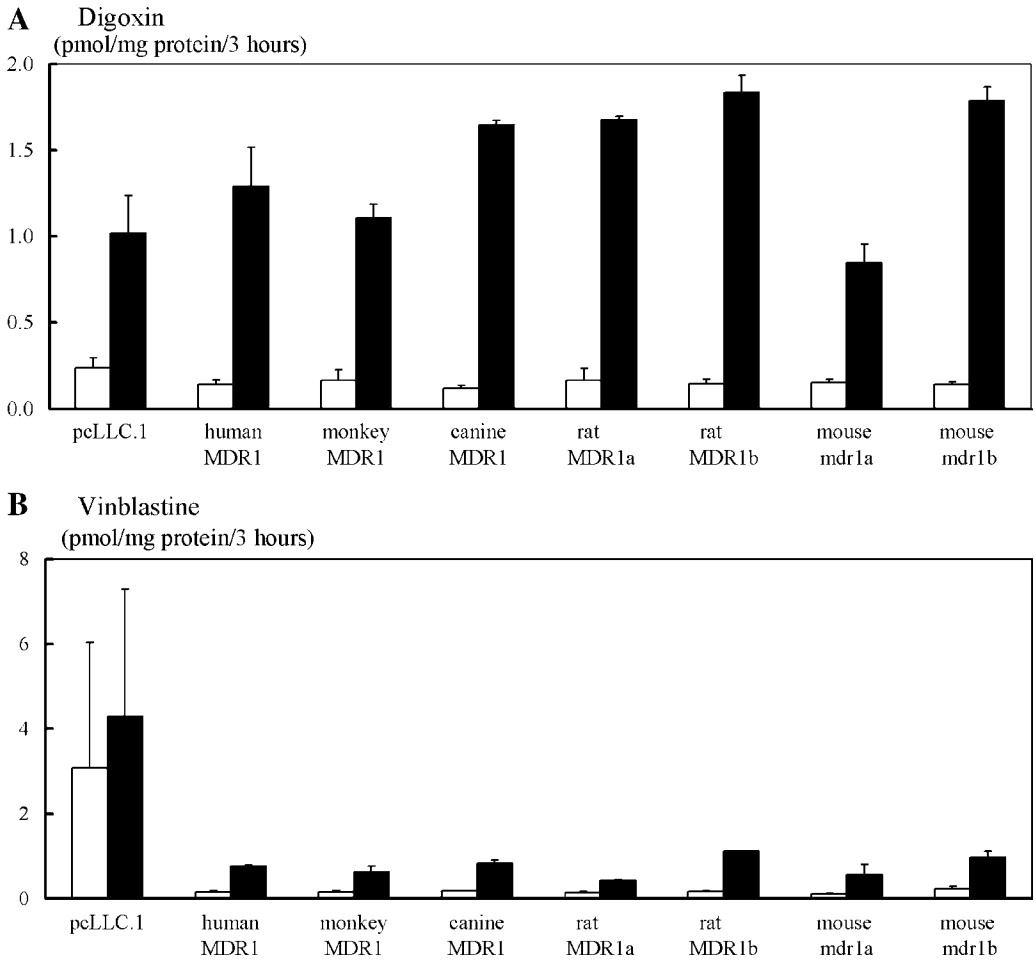

Fig. 5. Cellular accumulation of digoxin (A) and vinblastine (B) at 3 h in *MDR1* stably expressing derived from various animal species and pcLLC.1 cells. The concentrations of digoxin and vinblastine were 12.2 and 26.9 nmol L^{-1}, respectively. Open and closed columns represent the cellular accumulation of the compounds in A-to-B and B-to-A directions, respectively. Data are shown as mean ± SD ($n = 3-9$).

Interspecies and Interisoforms Correlation Analysis

To compare the interspecies and interisoforms efflux activities, a correlation analysis of the efflux ratio between various *MDR1* stably expressing cell lines was carried out. Figure 6 illustrates a summary of the correlation plots and Table V summarizes the correlation coefficient. There was a fairly good 1:1 correlation in the efflux ratio between human and monkey MDR1, rat MDR1b and mouse mdr1b, and mouse mdr1a and canine MDR1, indicating that the efflux activity of P-gp between human and monkey MDR1, rat MDR1b and mouse mdr1b, and mouse mdr1a and canine MDR1 was fairly consistent for the compounds tested. The efflux ratio for mdr1a and mdr1b derived from mouse and

Table II. Effect of Verapamil on the Transcellular Transport of Digoxin Across the Human *MDR1* Stably Expressing and pcLLC.1 Cells

	Human MDR1			pcLLC.1		
Verapamil (μmol L^{-1})	$PS_{A\text{-to-}B}$ (μL min^{-1} mg $protein^{-1}$)	$PS_{B\text{-to-}A}$ (μL min^{-1} mg $protein^{-1}$)	Efflux ratio	$PS_{A\text{-to-}B}$ (μL min^{-1} mg $protein^{-1}$)	$PS_{B\text{-to-}A}$ (μL min^{-1} mg $protein^{-1}$)	Efflux ratio
0	1.35 ± 0.11	9.34 ± 1.02	6.9	2.09 ± 1.16	3.31 ± 1.37	1.6
12.5	3.55 ± 0.22	9.92 ± 1.04	2.8	2.38 ± 0.18	2.50 ± 0.23	1.1
25	4.33 ± 0.40	7.04 ± 1.11	1.6	2.55 ± 0.04	2.70 ± 0.14	1.1
50	4.59 ± 0.46	5.50 ± 1.43	1.2	2.42 ± 0.19	3.01 ± 0.32	1.2

$PS_{A\text{-to-}B}$ and $PS_{B\text{-to-}A}$ were calculated by dividing transport amount from A-to-B and B-to-A directions, respectively, by incubation time and initial concentration of digoxin. The efflux ratio was calculated by dividing $PS_{B\text{-to-}A}$ by $PS_{A\text{-to-}B}$. The concentration of digoxin was 12.2 nmol L^{-1}. Results are shown as mean ± SD ($n = 3$).

Table III. Kinetic Parameters for Penetration Across *MDR1* Stably Expressing from Various Animal Species and pcLLC.1 Cells

Compounds	$PS_{A\text{-}to\text{-}B}$ ($\mu L\ min^{-1}$ mg protein^{-1})	$PS_{B\text{-}to\text{-}A}$ ($\mu L\ min^{-1}$ mg protein^{-1})	Efflux ratio	Corrected efflux ratio	$PS_{A\text{-}to\text{-}B}$ ($\mu L\ min^{-1}$ mg protein^{-1})	$PS_{B\text{-}to\text{-}A}$ ($\mu L\ min^{-1}$ mg protein^{-1})	Efflux ratio	Corrected efflux ratio
		pcLLC.1				Human MDR1		
Clarithromycin	0.04 ± 0.01	0.08 ± 0.01	1.8	–	0.01 ± 0.00	0.14 ± 0.01	22.1	12.3
Daunorubicin	1.27 ± 0.09	1.41 ± 0.09	1.1	–	1.54 ± 0.14	13.17 ± 1.18	8.5	7.7
Digoxin	2.28 ± 0.40	3.51 ± 0.50	1.5	–	0.60 ± 0.11	9.17 ± 1.77	15.3	10.2
Erythromycin	0.0009 ± 0.0000	0.0044 ± 0.0005	5.0	–	0.0005 ± 0.0001	0.0039 ± 0.0005	8.1	1.6
Etoposide	0.21 ± 0.02	0.21 ± 0.01	1.0	–	0.22 ± 0.02	0.92 ± 0.08	4.1	4.1
Paclitaxel	0.81 ± 0.10	4.78 ± 1.59	5.9	–	0.45 ± 0.13	13.64 ± 3.45	30.5	5.2
Propranolol	4.70 ± 0.93	6.29 ± 0.52	1.3	–	14.21 ± 0.76	16.01 ± 1.11	1.1	0.8
Quinidine	29.94 ± 1.83	13.15 ± 1.49	0.4	–	15.29 ± 5.49	23.02 ± 1.63	1.5	3.8
Ritonavir	2.37 ± 0.51	4.46 ± 0.67	1.9	–	0.81 ± 0.38	8.28 ± 1.66	10.2	5.4
Saquinavir	2.46 ± 0.32	4.59 ± 1.01	1.9	–	1.04 ± 0.14	5.52 ± 1.89	5.3	2.8
Verapamil	32.27 ± 3.07	15.54 ± 8.33	0.5	–	8.96 ± 1.01	29.02 ± 4.54	3.2	6.4
Vinblastine	1.63 ± 0.77	5.36 ± 1.27	3.3	–	0.60 ± 0.37	7.57 ± 0.46	12.5	3.8
		Monkey MDR1				Canine MDR1		
Clarithromycin	0.01 ± 0.00	0.13 ± 0.01	17.1	9.5	0.02 ± 0.01	0.19 ± 0.04	10.1	5.6
Daunorubicin	2.09 ± 0.18	10.13 ± 0.45	4.8	4.4	1.18 ± 0.59	8.17 ± 0.59	6.9	6.3
Digoxin	1.15 ± 1.13	12.74 ± 1.11	11.1	7.4	0.57 ± 0.24	15.62 ± 1.69	27.3	18.2
Erythromycin	0.0007 ± 0.0005	0.0044 ± 0.0010	6.2	1.2	0.0013 ± 0.0010	0.0066 ± 0.0006	5.0	1.0
Etoposide	0.37 ± 0.04	1.20 ± 0.04	3.3	3.3	0.49 ± 0.01	0.98 ± 0.05	2.0	2.0
Paclitaxel	0.31 ± 0.01	8.54 ± 2.55	27.1	4.6	0.59 ± 0.06	13.62 ± 0.98	22.9	3.9
Propranolol	7.85 ± 1.87	13.31 ± 1.94	1.7	1.3	5.91 ± 1.14	8.68 ± 0.1	1.5	1.2
Quinidine	9.46 ± 1.82	27.41 ± 7.56	2.9	7.3	12.32 ± 3.08	40.28 ± 6.51	3.3	8.3
Ritonavir	1.03 ± 0.23	3.21 ± 1.19	3.1	1.6	1.45 ± 0.83	12.15 ± 5.29	8.4	4.4
Saquinavir	0.96 ± 0.20	2.68 ± 1.07	2.8	1.5	0.87 ± 0.03	7.43 ± 2.45	8.5	4.5
Verapamil	5.02 ± 0.54	20.96 ± 3.76	4.2	8.4	7.74 ± 0.48	32.49 ± 10.64	4.2	8.4
Vinblastine	0.65 ± 0.55	8.83 ± 1.55	13.5	4.1	0.40 ± 0.04	11.78 ± 0.55	29.4	8.9
		Rat MDR1a				Rat MDR1b		
Clarithromycin	0.01 ± 0.00	0.17 ± 0.04	20.2	11.2	0.01 ± 0.01	0.15 ± 0.02	10.9	6.1
Daunorubicin	3.41 ± 0.18	13.17 ± 1.54	3.9	3.5	2.04 ± 0.36	9.13 ± 0.68	4.5	4.1
Digoxin	0.63 ± 0.05	13.10 ± 1.75	20.9	13.9	0.81 ± 0.04	15.63 ± 0.56	19.4	12.9
Erythromycin	0.0006 ± 0.0004	0.0055 ± 0.0012	8.9	1.8	0.0005 ± 0.0000	0.0067 ± 0.0002	13.9	2.8
Etoposide	1.77 ± 0.30	2.75 ± 0.75	1.6	1.6	0.31 ± 0.05	1.25 ± 0.11	4.0	4.0
Paclitaxel	0.87 ± 0.57	12.85 ± 2.28	14.8	2.5	0.73 ± 0.03	12.45 ± 2.11	17.2	2.9
Propranolol	12.86 ± 1.00	18.57 ± 0.21	1.4	1.1	12.76 ± 0.21	17.36 ± 1.49	1.4	1.1
Quinidine	11.10 ± 1.50	39.43 ± 20.02	3.6	9.0	13.39 ± 1.63	36.78 ± 6.31	2.7	6.8
Ritonavir	0.73 ± 0.22	11.06 ± 4.50	15.2	8.0	1.10 ± 0.59	13.17 ± 4.67	12.0	6.3
Saquinavir	1.19 ± 0.85	5.68 ± 1.26	4.8	2.5	1.22 ± 0.49	6.35 ± 2.32	5.2	2.7
Verapamil	9.55 ± 1.34	23.05 ± 7.63	2.4	4.8	10.20 ± 1.51	36.84 ± 17.00	3.6	7.2
Vinblastine	0.30 ± 0.05	5.56 ± 0.19	18.4	5.6	0.53 ± 0.04	8.40 ± 0.53	15.9	4.8
		Mouse mdr1a				Mouse mdr1b		
Clarithromycin	0.01 ± 0.01	0.15 ± 0.01	11.1	6.2	0.02 ± 0.01	0.16 ± 0.03	8.4	4.7
Daunorubicin	1.95 ± 0.18	11.04 ± 0.64	5.7	5.2	1.41 ± 0.05	7.31 ± 0.54	5.2	4.7
Digoxin	0.58 ± 0.16	12.67 ± 2.38	21.7	14.5	0.68 ± 0.08	15.61 ± 1.16	23.1	15.4
Erythromycin	0.0005 ± 0.0000	0.0045 ± 0.0002	8.7	1.7	0.0006 ± 0.0000	0.0058 ± 0.0009	10.1	2.0
etoposide	0.35 ± 0.05	1.03 ± 0.01	3.0	3.0	0.25 ± 0.01	1.01 ± 0.02	4.0	4.0
Paclitaxel	0.67 ± 0.22	12.33 ± 0.74	18.4	3.1	0.78 ± 0.23	14.40 ± 5.76	18.5	3.1
Propranolol	9.13 ± 0.62	12.66 ± 0.86	1.4	1.1	10.34 ± 1.42	15.18 ± 1.24	1.5	1.2
Quinidine	15.64 ± 1.05	18.78 ± 0.86	1.2	3.0	16.20 ± 2.83	19.54 ± 0.43	1.2	3.0
Ritonavir	0.81 ± 0.12	4.79 ± 2.23	5.9	3.1	0.84 ± 0.21	4.85 ± 1.33	5.7	3.0
Saquinavir	1.13 ± 0.08	3.70 ± 0.93	3.3	1.7	0.88 ± 0.28	4.03 ± 0.33	4.6	2.4
Verapamil	10.98 ± 0.35	17.92 ± 3.40	1.6	3.2	10.07 ± 0.84	16.74 ± 4.86	1.7	3.4
Vinblastine	0.28 ± 0.04	9.24 ± 3.65	33.6	10.2	0.71 ± 0.45	9.88 ± 0.82	13.8	4.2

Based on the representative results shown in Figs. 3 and 4, A-to-B and B-to-A of the PS product, efflux ratio, and corrected efflux ratio across *MDR1* stably expressing and pcLLC.1 cells were calculated. $PS_{A\text{-}to\text{-}B}$ and $PS_{B\text{-}to\text{-}A}$ were calculated by dividing transport amount from A-to-B and B-to-A, respectively, by incubation time and initial concentrations of the compounds. Efflux ratio was calculated by dividing $PS_{B\text{-}to\text{-}A}$ by $PS_{A\text{-}to\text{-}B}$. Corrected efflux ratio was calculated by dividing the efflux ratio for *MDR1* stably expressing cells by that for pcLLC.1. All parameters are calculated from the time point when permeable amounts increased linearly. Concentrations of compounds ranged from 2.2 nmol L^{-1} to 5.1 μmol L^{-1}. Results are shown as mean ± SD (n = 3–9).

Table IV. Cellular Accumulation of 12 Compounds at 3 h in *MDR1* Stably Expressing from Various Animal Species and pcLLC.1 Cells

Compounds	Concentration (nmol L^{-1})	A-to-B (μL mg protein^{-1})	B-to-A (μL mg protein^{-1})	A-to-B (μL mg protein^{-1})	B-to-A (μL mg protein^{-1})
		pcLLC.1		Human MDR1	
Clarithromycin	5,025	0.29 ± 0.01	0.44 ± 0.05	0.03 ± 0.00	0.06 ± 0.01
Daunorubicin	36.7	558.58 ± 38.42	668.94 ± 21.53	25.89 ± 1.91	68.94 ± 7.90
Digoxin	12.2	19.51 ± 4.59	83.44 ± 17.87	11.80 ± 2.13	105.82 ± 18.44
Erythromycin	5,100	0.011 ± 0.001	0.032 ± 0.003	0.003 ± 0.000	0.003 ± 0.000
Etoposide	5,120	0.77 ± 0.06	1.55 ± 0.31	0.64 ± 0.09	0.96 ± 0.11
Paclitaxel	3.9	762.56 ± 51.54	1,767.18 ± 170.26	23.08 ± 3.85	126.92 ± 21.28
Propranolol	48.2	75.31 ± 18.46	154.15 ± 16.39	115.77 ± 5.81	218.26 ± 14.32
Quinidine	10.1	72.67 ± 3.76	154.46 ± 17.82	120.50 ± 13.96	212.38 ± 5.54
Ritonavir	62.7	40.94 ± 11.26	42.82 ± 6.60	8.02 ± 2.82	17.88 ± 1.87
Saquinavir	69.9	13.89 ± 1.89	26.02 ± 5.05	5.11 ± 1.13	12.63 ± 3.25
Verapamil	2.2	169.55 ± 42.73	339.09 ± 59.09	150.91 ± 17.73	401.82 ± 15.91
Vinblastine	26.9	114.30 ± 109.91	159.33 ± 111.69	5.72 ± 1.19	28.36 ± 0.86
		Monkey MDR1		Canine MDR1	
Clarithromycin	5,025	0.04 ± 0.01	0.05 ± 0.01	0.03 ± 0.00	0.03 ± 0.00
Daunorubicin	36.7	22.07 ± 4.36	49.32 ± 5.18	23.71 ± 8.17	56.95 ± 4.36
Digoxin	12.2	13.44 ± 5.16	90.74 ± 6.64	9.67 ± 1.48	135.00 ± 2.13
Erythromycin	5,100	0.007 ± 0.001	0.003 ± 0.000	0.004 ± 0.001	0.002 ± 0.001
Etoposide	5,120	2.77 ± 0.47	0.94 ± 0.09	1.23 ± 0.23	0.52 ± 0.08
Paclitaxel	3.9	22.56 ± 0.51	73.33 ± 12.31	26.41 ± 5.38	90.77 ± 1.54
Propranolol	48.2	218.67 ± 7.47	400.62 ± 12.24	252.70 ± 11.20	387.55 ± 14.32
Quinidine	10.1	79.50 ± 8.91	130.89 ± 16.04	52.67 ± 17.52	94.85 ± 2.77
Ritonavir	62.7	12.39 ± 0.53	10.85 ± 2.65	9.47 ± 1.90	19.25 ± 9.74
Saquinavir	69.9	6.55 ± 0.86	9.56 ± 2.20	2.80 ± 0.80	7.75 ± 1.02
Verapamil	2.2	65.91 ± 6.82	145.00 ± 10.45	66.82 ± 9.09	161.36 ± 56.36
Vinblastine	26.9	5.80 ± 1.30	23.35 ± 5.24	6.80 ± 0.37	30.89 ± 2.79
		Rat MDR1a		Rat MDR1b	
Clarithromycin	5,025	0.03 ± 0.00	0.05 ± 0.00	0.04 ± 0.01	0.05 ± 0.00
Daunorubicin	36.7	22.34 ± 1.91	39.24 ± 3.81	25.61 ± 6.54	61.04 ± 3.00
Digoxin	12.2	13.61 ± 5.57	137.54 ± 1.48	11.97 ± 2.13	150.25 ± 8.11
Erythromycin	5,100	0.005 ± 0.001	0.002 ± 0.000	0.006 ± 0.001	0.003 ± 0.001
Etoposide	5,120	3.97 ± 1.18	1.55 ± 0.03	1.66 ± 0.36	0.84 ± 0.07
Paclitaxel	3.9	26.15 ± 2.31	95.13 ± 13.85	27.69 ± 2.56	99.49 ± 6.15
Propranolol	48.2	193.57 ± 11.00	331.95 ± 52.49	133.20 ± 3.73	243.78 ± 33.82
Quinidine	10.1	44.16 ± 4.26	78.71 ± 22.57	51.09 ± 9.90	97.72 ± 13.76
Ritonavir	62.7	8.47 ± 1.71	21.69 ± 7.40	8.53 ± 1.55	19.68 ± 10.05
Saquinavir	69.9	3.62 ± 1.26	8.80 ± 1.36	6.37 ± 2.65	9.34 ± 3.73
Verapamil	2.2	67.27 ± 15.91	135.00 ± 25.00	67.27 ± 16.82	165.00 ± 43.18
Vinblastine	26.9	5.24 ± 0.93	15.72 ± 1.15	6.32 ± 0.45	41.19 ± 0.67
		Mouse mdr1a		Mouse mdr1b	
Clarithromycin	5,025	0.03 ± 0.00	0.05 ± 0.00	0.05 ± 0.00	0.08 ± 0.01
Daunorubicin	36.7	39.51 ± 10.08	66.21 ± 0.54	24.52 ± 8.17	38.42 ± 4.90
Digoxin	12.2	12.38 ± 1.64	69.34 ± 8.93	11.64 ± 0.98	146.39 ± 6.64
Erythromycin	5,100	0.005 ± 0.001	0.004 ± 0.000	0.005 ± 0.000	0.003 ± 0.000
Etoposide	5,120	1.04 ± 0.01	0.97 ± 0.03	1.32 ± 0.16	0.65 ± 0.26
Paclitaxel	3.9	40.77 ± 11.03	105.13 ± 3.08	37.18 ± 7.95	119.23 ± 34.10
Propranolol	48.2	172.20 ± 7.88	328.63 ± 13.69	132.57 ± 19.09	295.85 ± 24.27
Quinidine	10.1	76.63 ± 9.11	144.16 ± 35.54	75.84 ± 5.84	137.03 ± 13.66
Ritonavir	62.7	5.68 ± 1.67	11.58 ± 2.92	7.50 ± 1.66	13.21 ± 1.99
Saquinavir	69.9	5.35 ± 1.33	8.21 ± 1.60	6.64 ± 2.76	8.83 ± 3.00
Verapamil	2.2	131.82 ± 10.91	230.45 ± 15.45	112.27 ± 22.73	213.18 ± 49.55
Vinblastine	26.9	4.42 ± 0.41	20.78 ± 8.88	8.62 ± 1.93	35.84 ± 5.72

C/M ratios of A-to-B and B-to-A directions were calculated by dividing accumulation amount from A-to-B and B-to-A, respectively, by initial concentration of compounds. Results are shown as mean ± SD (n = 3–9).

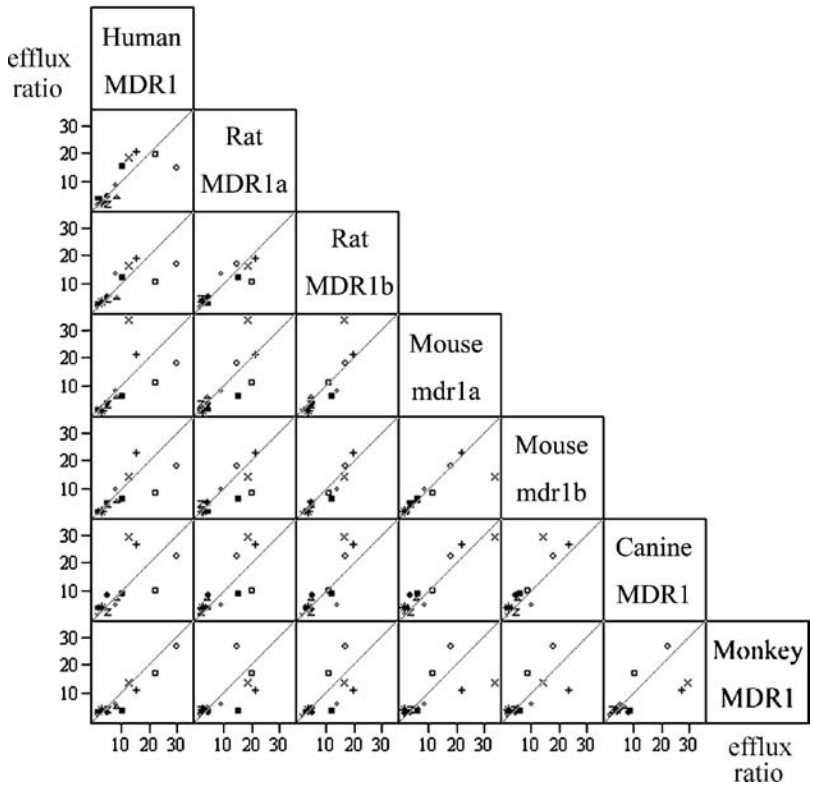

Fig. 6. Correlation of the efflux ratio between *MDR1* stably expressing cells from various animal species. Based on the results shown in Table III, a correlation analysis of the efflux ratio between *MDR1* stably expressing cells from various animal species was done, and the results are shown. □, Clarithromycin; △, daunorubicin; +, digoxin; ◇, erythromycin; z, etoposide; ○, paclitaxel; Y, propranolol; ▬, quinidine; ■, ritonavir; •, saquinavir; *, verapamil; ×, vinblastine.

rat also comparatively correlate well. On the other hand, the correlation exhibited a substantial difference between human MDR1 and mouse mdr1a, human and canine MDR1, rat MDR1a and monkey MDR1, mouse mdr1a and monkey MDR1, and canine and monkey MDR1. Correlation analysis for the corrected efflux ratio between various *MDR1* stably expressing cell lines was also examined (data not shown). Because the results of analysis for the corrected efflux ratio were similar to those for the efflux ratio, we adopted the efflux ratio as a parameter for a simple analytical method.

DISCUSSION

The cellular strain LLC-PK_1 forms a highly polarized epithelium, and polarized transport of nutrients and xenobiotics across cultured epithelia has been reported (23–26). Little activity attributable to MDR1 in this strain made it suitable as an expression donor of this efflux transporter (27), and heterogeneously expressed *MDR1* in the LLC-PK_1 was specifically localized on the apical surface of the cells (19,20). Utilizing these characteristics, we expressed *MDR1* from various animal species in LLC-PK_1, and conducted trans-

Table V. Correlation Coefficients of the Efflux Ratio between *MDR1* Stably Expressing Cells from Various Animal Species

	Human MDR1	Rat MDR1a	Rat MDR1b	Mouse mdr1a	Mouse mdr1b	Canine MDR1
Rat MDR1a	0.762	1				
Rat MDR1b	0.753	0.886	1			
Mouse mdr1a	0.609	0.786	0.828	1		
Mouse mdr1b	0.748	0.789	0.931	0.822	1	
Canine MDR1	0.665	0.794	0.842	0.948	0.888	1
Monkey MDR1	0.954	0.680	0.701	0.669	0.729	0.697

Based on results shown in Table III, a correlation analysis of the efflux ratio between *MDR1* stably expressing cells from various animal species was done, and the correlation coefficients are shown.

cellular transport studies for clarithromycin, daunorubicin, digoxin, erythromycin, etoposide, paclitaxel, propranolol, quinidine, ritonavir, saquinavir, verapamil, and vinblastine. Variety in the PS product was observed between the compounds, and was considered to depend on membrane permeability resulting from the physicochemical properties of the compounds. Except for propranolol and erythromycin, all compounds showed high permeability in the B-to-A direction in all *MDR1* expressing cells compared with that in the pcLLC.1 cells. This transport characteristic of the compounds was the same as that reported previously (14,21,22,28). Directional transport of some compounds was also observed in pcLLC.1; in particular, the B-to-A transport for erythromycin, paclitaxel, and vinblastine was larger than in the opposite direction. A similar tendency for vinblastine in LLC-PK_1 was also observed previously (14,22,27). In contrast, the A-to-B transport for quinidine and verapamil was larger than that in the opposite direction. These characteristics are considered to be attributable to transport activity by endogenous transporters in the LLC-PK_1 cells (27,29). Thus, comparison of the transcellular transport by pcLLC.1 cells is necessary in experiments using *MDR1*-expressing cells.

Variety was also observed for accumulation of compounds in the cells. One possible explanation for the differences in C/M ratios may be attributed to differences in intracellular binding. The accumulation of vinblastine, paclitaxel, clarithromycin, erythromycin, and daunorubicin in all *MDR1* expressing cells was low compared with that in pcLLC.1 cells. Values of C/M ratio for paclitaxel, daunorubicin, and vinblastine in pcLLC.1 cells at 3 h ranged approximately from 16- to 253-fold higher than the intracellular volume of LLC-PK_1 cells at 7.0 μL mg protein^{-1} (30). Although the accumulation of several compounds including digoxin, etoposide, and quinidine was not different between *MDR1* expressing cells and pcLLC.1 cells, the C/M ratio for many of these compounds was relatively low. A similar tendency for digoxin was also previously observed (21). The concentration in the cells may permit the detection of efflux activity from the point of cellular accumulation. Thus, all the compounds examined in this study, except for propranolol, showed efflux activity with regard to transcellular transport and/or accumulation in all *MDR1* stably expressing cells as compared with that in pcLLC.1 cells, and were judged to be substrates of P-gps. Directional transport of propranolol was not observed in Caco-2 cells and the compound is considered to be a poor substrate for P-gp (31). It is also reported that P-gp-mediated efflux activity may be saturated more readily when the substrate approaches from the basolateral side rather than the apical side (32). As P-gp is localized on the apical membrane of Caco-2 cells, entry of cells from the apical side may be difficult compared with that from the basolateral side. The accumulation of almost all compounds examined in this study in all cells from A-to-B direction tended to be less than that from the opposite direction, suggesting that the P-gps in this study are located on the apical surface of the membrane. Results of the inhibitory effects of verapamil were put into consideration; we finally concluded the establishment of transformants stably expressing *MDR1* for seven strains from five animal species.

The objective of this study was to examine the species difference of P-gp in terms of efflux activity by using *MDR1* stably expressing cells. However, the species difference for efflux activity was not particularly high with the 12 compounds examined. Therefore, a correlation analysis of the efflux ratio between two animal species was performed. It has been reported that the efflux ratio at one substrate concentration cannot assess how P-gp-mediated efflux activity attenuates absorption and enhances secretory transport of P-gp substrates across a polarized epithelium (32). However, efflux ratio would be a useful parameter for exhaustive comparison because this parameter gives an intrinsic value to each compound at a low substrate concentration. Because the substrate concentrations used in this study and the K_m values of B-to-A transport reported in the transport experiments (33) ranged from 2.2 nmol L^{-1} to 5.1 μmol L^{-1} and from 3.8 to 213 μmol L^{-1}, respectively, the efflux ratio for all tested compounds is considered to be calculated in a concentration range without saturation of efflux activity. Moreover, for discussion of species differences in the efflux activity of P-gp using the simple comparison of the efflux ratio obtained from cell lines, Yamazaki *et al.* (14) pointed out that the efflux activity of P-gp could be affected by at least two factors: total protein expression and density of the functional transporter in each cell line. Thus, we also evaluated the transport activity normalized by total protein concentration for adjustment of the passive permeability of each cell line. The density of the transporter is considered to affect the slope of the correlation. However, our results representing human MDR1 *vs.* mouse mdr1a, human *vs.* canine MDR1, and monkey MDR1 *vs.* mouse mdr1a (Fig. 6) show that several compounds deviate from both sides of the 1:1 correlation line. Even though the slopes for the plots in those species change, it does not improve the correlation. Therefore, the deviation in the correlation is considered to be attributable to species differences in P-gp.

The tendency toward poor correlation between the human MDR1 and mouse mdr1a corresponded to previously reported results (14). Interestingly, the efflux ratio with human and monkey MDR1 exhibits a fairly good correlation. It is well known that pharmacokinetic parameters for humans and monkeys are quite different (34). For example, because the metabolic clearances and hepatic enzyme activities in monkeys are higher compared to humans, BA values in monkeys are considered to be different. However, monkeys and humans seem to be generally similar with regard to the rate and extent of drug absorption (34). Therefore, the monkey may be a good model for prediction of the efflux activity derived by P-gp in humans. In addition, high homology of the amino acid sequences between the species (96% for the human and monkey MDR1) may be one of the factors responsible for determining the similarity of efflux activity.

Our ultimate goal is to estimate P-gp contribution in humans for the research and development of a new drug. However, pharmacokinetic parameters are determined by complicated disposition processes. In particular, if a compound is effectively metabolized, it is not easy to estimate P-gp contribution by separating the transport and metabolism processes. Because there is little metabolic activity in LLC-PK_1 (35), the established transformants can be used to

evaluate the transport activity among the species without considering the contribution of metabolism. On the other hand, to discuss the *in vitro–in vivo* relations of the efflux activities, it is necessary to note the following points. First, there are no data on the differences in glycosylation between the stably *MDR1* expressing cells and in the tissues. However, the ATP-binding domains and intracellular flexible linker loops of P-gp play a key role in the transport activity (36), and the absence of *N*-glycosylation did not alter the level or pattern of (cross-) resistance (37). Even though glycosylation in *MDR1* stably expressing cells is not equivalent to that in the tissues, this difference will not largely affect the transport activity of the substrates. Second, the expression level between the established stably expressing *MDR1* cells and in the tissues of each animal may not be similar. Although we confirmed the expression of the P-gp in each cell line determined by C219 monoclonal antibody shown in Fig. 2, we could not elucidate the degree of cross-reactivity of the antibody to each P-gp. Therefore the expression level of P-gps in each cell line remains unclear. It is necessary to establish the methodology of quantifying P-gp over the species.

In conclusion, we established transformants stably expressing *MDR1* for seven strains from five animal species in LLC-PK_1. These cells are considered to be useful as powerful tools for P-gp substrate identification studies and for clarifying the clinical and nonclinical pharmacokinetics of compounds. In addition, our results show that the interspecies differences and similarities of P-gp may reflect the substrate efflux activity.

ACKNOWLEDGMENTS

We are deeply thankful to Professor Dr. Yusuke Tanigawara, Keio University, and Professor Dr. Kazumitsu Ueda, Kyoto University, for supplying LLC-GA5-COL300 cells as a positive control to establish the *MDR1* stably expressing cells.

REFERENCES

1. R. L. Juliano and V. Ling. A surface glycoprotein modulating drug permeability in Chinese hamster ovary cell mutants. *Biochim. Biophys. Acta* **455**:152–162 (1976).
2. F. Thiebaut, T. Tsuruo, H. Hamada, M. M. Gottesman, I. Pastan, and M. C. Willingham. Cellular localization of the multidrug-resistance gene product P-glycoprotein in normal human tissues. *Proc. Natl. Acad. Sci. USA* **84**:7735–7738 (1987).
3. C. J. Matheny, M. W. Lamb, K. R. Brouwer, and G. M. Pollack. Pharmacokinetic and pharmacodynamic implications of P-glycoprotein modulation. *Pharmacotherapy* **21**:778–796 (2001).
4. A. Sparreboom, J. van Asperen, U. Mayer, A. H. Schinkel, J. W. Smit, D. K. Meijer, P. Borst, W. J. Nooijen, J. H. Beijnen, and O. van Tellingen. Limited oral bioavailability and active epithelial excretion of paclitaxel (Taxol) caused by P-glycoprotein in the intestine. *Proc. Natl. Acad. Sci. USA* **94**:2031–2035 (1997).
5. M. Sababi, O. Borga, and U. Hultkvist-Bengtsson. The role of P-glycoprotein in limiting intestinal regional absorption of digoxin in rats. *Eur. J. Pharm. Sci.* **14**:21–27 (2001).
6. L. M. Chan, S. Lowes, and B. H. Hirst. The ABCs of drug transport in intestine and liver: efflux proteins limiting drug absorption and bioavailability. *Eur. J. Pharm. Sci.* **21**:25–51 (2004).
7. M. F. Fromm, R. B. Kim, C. M. Stein, G. R. Wilkinson, and D. M. Roden. Inhibition of P-glycoprotein-mediated drug transport: a unifying mechanism to explain the interaction between digoxin and quinidine. *Circulation* **99**:552–557 (1999).
8. B. Greiner, M. Eichelbaum, P. Fritz, H. P. Kreichgauer, O. Von Richter, J. Zundler, and H. K. Kroemer. The role of intestinal P-glycoprotein in the interaction of digoxin and rifampin. *J. Clin. Invest.* **104**:147–153 (1999).
9. A. Harrison, A. Betts, K. Fenner, K. Beaumont, A. Edgington, S. Roffey, J. Davis, P. Comby, and P. Morgan. Nonlinear oral pharmacokinetics of the α-antagonist 4-amino-5-(4-fluorophenyl)-6,7-dimethoxy-2-[4-(morpholinocarbonyl)-perhydro-1,4-diazepin-1-yl]quinoline in humans: use of preclinical data to rationalize clinical observations. *Drug Metab. Dispos.* **32**:197–204 (2004).
10. A. H. Schinkel, J. J. Smit, O. van Tellingen, J. H. Beijnen, E. Wagenaar, L. van Deemter, C. A. Mol, M. A. van der Valk, E. C. Robanus-Maandag, H. P. Rielete, A. J. M. Berns, and P. Borst. Disruption of the mouse mdr1a P-glycoprotein gene leads to a deficiency in the blood–brain barrier and to increased sensitivity to drugs. *Cell* **77**:491–502 (1994).
11. A. H. Schinkel, U. Mayer, E. Wagenaar, C. A. Mol, L. van Deemter, J. J. Smit, M. A. van der Valk, A. C. Voordouw, H. Spits, O. van Tellingen, J. M. Zijlmans, W. E. Fibbe, and P. Borst. Normal viability and altered pharmacokinetics in mice lacking mdr1-type (drug-transporting) P-glycoproteins. *Proc. Natl. Acad. Sci. USA* **94**:4028–4033 (1997).
12. M. M. Gottesman and I. Pastan. Biochemistry of multidrug resistance mediated by the multidrug transporter. *Annu. Rev. Biochem.* **62**:385–427 (1993).
13. D. F. Tang-Wai, S. Kajiji, F. DiCapua, D. Graafde, I. B. Roninson, and P. Gros. Human (MDR1) and mouse (mdr1, mdr3) P-glycoproteins can be distinguished by their respective drug resistance profiles and sensitivity to modulators. *Biochemistry* **34**:32–39 (1995).
14. M. Yamazaki, W. E. Neway, T. Ohe, I. Chen, J. F. Rowe, J. H. Hochman, M. Chiba, and J. H. Lin. *In vitro* substrate identification studies for P-glycoprotein-mediated transport: species difference and predictability of *in vivo* results. *J. Pharmacol. Exp. Ther.* **296**:723–735 (2001).
15. S. Kumar, G. Y. Kwei, G. K. Poon, S. A. Iliff, Y. Wang, Q. Chen, R. B. Franklin, V. Didolkar, R. W. Wang, M. Yamazaki, S. H. Chiu, J. H. Lin, P. G. Pearson, and T. A. Baillie. Pharmacokinetics and interactions of a novel antagonist of chemokine receptor 5 (CCR5) with ritonavir in rats and monkeys: role of CYP3A and P-glycoprotein. *J. Pharmacol. Exp. Ther.* **304**:1161–1171 (2003).
16. D. K. Walker, S. Abel, P. Comby, G. J. Muirhead, A. N. R. Nedderman, and D. A. Smith. Species differences in the disposition of the CCR5 antagonist, UK-427,857, a new potential treatment for HIV. *Drug Metab. Dispos.* **33**:587–595 (2005).
17. D. K. Yu. The contribution of P-glycoprotein to pharmacokinetic drug–drug interactions. *J. Clin. Pharmacol.* **39**:1203–1211 (1999).
18. A. Tsuji. Transporter-mediated drug interactions. *Drug Metab. Pharmacokinet.* **17**:253–274 (2002).
19. Y. Tanigawara, N. Okamura, M. Hirai, M. Yasuhara, K. Ueda, N. Kioka, T. Komano, and R. Hori. Transport of digoxin by human P-glycoprotein expressed in a porcine kidney epithelial cell line (LLC-PK_1). *J. Pharmacol. Exp. Ther.* **263**:840–845 (1992).
20. K. Ueda, N. Okamura, M. Hirai, Y. Tanigawara, T. Saeki, N. Kioka, T. Komano, and R. Hori. Human P-glycoprotein transports cortisol, aldosterone, and dexamethasone, but not progesterone. *J. Biol. Chem.* **267**:24248–24252 (1992).
21. M. Katoh, M. Nakajima, H. Yamazaki, and T. Yokoi. Inhibitory potencies of 1,4-dihydropyridine calcium antagonists to P-glycoprotein-mediated transport: comparison with the effects on CYP3A4. *Pharm. Res.* **17**:1189–1197 (2000).
22. Y. Adachi, H. Suzuki, and Y. Sugiyama. Comparative studies on *in vitro* methods for evaluating *in vivo* function of MDR1 P-glycoprotein. *Pharm. Res.* **18**:1660–1668 (2001).

23. D. S. Misfeldt and M. J. Sanders. Transepithelial transport in cell culture: D-glucose transport by a pig kidney cell line (LLC-PK_1). *J. Membr. Biol.* **59**:13–18 (1981).
24. C. Fauth, B. Rossier, and F. Roch-Ramel. Transport of tetraethylammonium by a kidney epithelial cell line (LLC-PK_1). *Am. J. Physiol.* **254**:F351–F357 (1988).
25. A. K. Fouda, C. Fauth, and F. Roch-Ramel. Transport of organic cations by kidney epithelial cell line LLC-PK_1. *J. Pharmacol. Exp. Ther.* **252**:286–292 (1990).
26. A. Takayama, Y. Okazaki, K. Fukuda, M. Takano, K. Inui, and R. Hori. Transport of cyclosporin A in kidney epithelial cell line (LLC-PK_1). *J. Pharmacol. Exp. Ther.* **257**:200–204 (1991).
27. L. B. Goh, K. J. Spears, D. Yao, A. Ayrton, P. Morgan, C. R. Wolf, and T. Friedberg. Endogenous drug transporters in *in vitro* and *in vivo* models for the prediction of drug disposition in man. *Biochem. Pharmacol.* **64**:1569–1578 (2002).
28. C. Chen, X. Liu, and B. J. Smith. Utility of *mdr1*-gene deficient mice in assessing the impact of P-glycoprotein on pharmacokinetics and pharmacodynamics in drug discovery and development. *Curr. Drug. Metab.* **4**:272–291 (2003).
29. U. Wenzel, D. Diehl, M. Herget, and H. Daniel. Endogenous expression of the renal high-affinity H^+-peptide cotransporter in LLC-PK_1 cells. *Am. J. Physiol.* **275**:C1573–C1579 (1998).
30. H. Saito, K. Inui, and R. Hori. Mechanisms of gentamicin transport in kidney epithelial cell line (LLC-PK_1). *J. Pharmacol. Exp. Ther.* **238**:1071–1076 (1986).
31. A. Collett, J. Tanianis-Hughes, and G. Warhurst. Rapid induction of P-glycoprotein expression by high permeability compounds in colonic cells *in vitro*: a possible source of transporter mediated drug interactions? *Biochem. Pharmacol.* **68**:783–790 (2004).
32. M. D. Troutman and D. R. Thakker. Efflux ratio cannot assess P-glycoprotein-mediated attenuation of absorptive transport: asymmetric effect of P-glycoprotein on absorptive and secretory transport across Caco-2 cell monolayers. *Pharm. Res.* **20**: 1200–1209 (2003).
33. J. H. Lin and M. Yamazaki. Role of P-glycoprotein in pharmacokinetics. *Clin. Pharmacokinet.* **42**:59–98 (2003).
34. W. L. Chiou and P. W. Buehler. Comparison of oral absorption and bioavailability of drugs between monkey and human. *Pharm. Res.* **19**:868–874 (2002).
35. C. P. Siegers, S. Denker, B. Steffen, and W. Jelkmann. Biotransformation enzymes in two renal epithelial cell lines (LLC-PK_1 and RK-L). *Mol. Toxicol.* **1**:335–339 (1987).
36. J. J. Gribar, M. Ramachandra, C. A. Hrycyna, S. Dey, and S. V. Ambudkar. Functional characterization of glycosylation-deficient human P-glycoprotein using a vaccinia virus expression system. *J. Membr. Biol.* **173**:203–214 (2000).
37. A. H. Schinkel, S. Kemp, M. Dolle, G. Rudenko, and E. Wagenaar. *N*-Glycosylation and deletion mutants of the human *MDR1* P-glycoprotein. *J. Biol. Chem.* **268**:7474–7481 (1993).